Surface & Coatings Technology 204 (2009) 829–833

Contents lists available at ScienceDirect

Surface & Coatings Technology

journal homepage: www.elsevier.com/locate/surfcoat

High temperature wear behavior of aluminum oxide layers produced by AC micro arc oxidation

E. Arslan [a,*], Y. Totik [b], E.E. Demirci [b], Y. Vangolu [b], A. Alsaran [b], I. Efeoglu [b]

[a] Erzurum College of Vocational Ataturk University 25240 Erzurum, Turkey
[b] Ataturk University, Department of Mechanical Engineering, Faculty of Engineering, Erzurum, Turkey

ARTICLE INFO

Available online 1 October 2009

Keywords:
Aluminum alloys
Micro arc oxidation
High temperature
Wear

ABSTRACT

Aluminum alloys are becoming increasingly important, especially in the automotive and aerospace industries. However, these materials tend to have poor wear resistance at atmospheric and high temperature conditions. Aluminum oxide layers are potentially very effective in developing hard, wear-resistant surfaces. The aim of present study was to evaluate the high temperature wear behavior of aluminum oxide layers at different temperatures by using high temperature pin-on-disc tribo tester and alumina balls as counterfaces. The aluminum oxide layers were produced by AC micro arc oxidation (MAO). The structural analyses of the layers were performed using XRD and SEM techniques. The hardness was measured using microhardness tester. The wear rates and friction coefficient was decreased with increasing wear test temperature. The lowest wear rate and friction coefficient, narrow and smooth wear tracks are obtained at 200 °C.

1. Introduction

Aluminum and its alloys are desirable materials due to high strength stiffness to weight ratio, good formability, good corrosion resistance, and recycling potential for use in automobile industries as components of internal combustion engines, e.g., cylinder blocks, cylinder heads and pistons [1]. These components are subject to high temperature during service. These alloys are susceptible to wear when matched to harder surfaces under high loads at elevated temperatures [2,3]. Some attempts have been made to overcome these problems of aluminum and its alloys by means of many surface engineering techniques such as chemical vapor deposition (CVD), physical vapor deposition (PVD), ion beam assisted deposition, thermal spraying and anodizing. Besides these, there has been increased interest to modify the surface properties of aluminum and its alloys by micro arc oxidation (MAO, also named as plasma electrolytic oxidation or anodic spark oxidation) in the recent years.

Micro arc oxidation (MAO) is a potential process to uniformly synthesize the ceramic-like oxide layers on aluminum by discharging sparks at a high voltage. This technique runs at potentials above the breakdown voltage of the oxide film growing on the surface of an aluminum anode by using high voltage, low frequency, AC supply in dilute alkaline electrolytes [4–6]. The oxide layers grown by MAO of aluminum alloys are thick (≈100 μm), hard and adherent to the substrate. The layers consist typically of porous top layer, dense intermediate layer and thin inner layer [2,7–13]. MAO is attracting increasing interest in fabricating ceramic-like coatings on aluminium, magnesium and titanium alloys, with the purpose of providing corrosion and wear resistance or various functional properties [5,14–19]. It is characterized by high productivity, economic efficiency, ecological friendliness, high hardness, good wear resistance, and excellent bonding strength with the substrate [5,20–24].

In the work reported here, a thick, hard layer is produced on AA2014 aluminum alloy using MAO at unipolar mode. The structural analysis of the layers is investigated using X-ray diffraction (XRD). Surface morphology and thickness of the layers are examined by SEM. Tribological tests are carried out at room temperature, 50 °C and 200 °C. The tribological performances of the layers were evaluated at room and high temperature.

2. Experimental

AA2014 aluminum alloys, whose chemical composition is given in Table 1, were used as the substrate material. Plate substrates with dimensions 25×25×4 mm were polished to a roughness of Ra≈0.1 μm, cleaned with acetone, ethanol and distilled water prior to MAO process. MAO treatment of the aluminum alloys was performed in the MAO-15 system designed and built by Plasma Technology Ltd. Aqueous solution of KOH, Na_2HPO_4 and Na_2SiO_3 was used as the electrolyte. Deionizing (DI) water was used to prepare the

Table 1
The chemical composition of AA 2014 substrate.

Material (wt.%)	Cu	Mg	Mn	Si	Fe	Cr	Sn
AA2014	5.0	0.68	0.58	0.83	0.23	0.04	0.03

* Corresponding author. Tel.: +90 442 2312649; fax: +90 442 2360982.
E-mail address: earslan@atauni.edu.tr (E. Arslan).

0257-8972/$ – see front matter © 2009 Elsevier B.V. All rights reserved.
doi:10.1016/j.surfcoat.2009.09.057

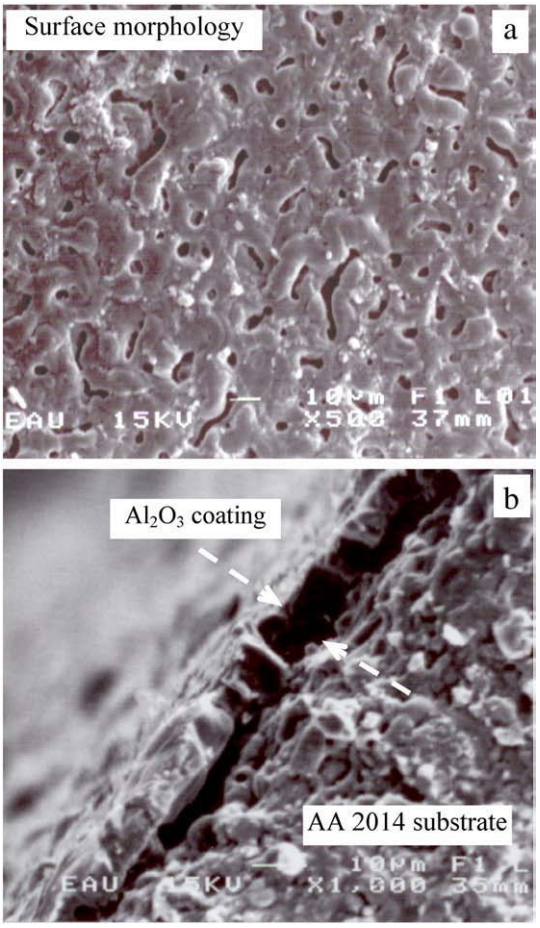

Fig. 1. SEM images of a) surface topography and b) cross section of the MAO Al_2O_3 layers.

aqueous solution. MAO process was carried out at unipolar mode with AC power supply. A unipolar mode at constant current of 1.2 A and 100 Hz was applied to substrate for 60 min. The unipolar process was performed at a 50% positive pulse duty cycle. The sample and stainless steel container walls were used as the anode and cathode, respectively. During the oxidation process, the electrolyte was stirred and cooled to prevent heating over 30 °C. After the MAO process, the oxidized samples were washed with distilled water and dried at room temperature.

The fractured cross-sections, oxide thickness and surface morphology of the layers at constant current using unipolar mode were analyzed by a scanning electron microscope (SEM-Jeol-6400). The microhardness of the samples was tested using a Buhler Microhardness Tester. The oxidized samples were polished using 0.05 μm diamond paste, before the measurement of hardness. At least five indentations at different places on the film surface were measured and averaged under 10 gf load for each sample.

Tribological properties at high temperatures of the layers were evaluated by a pin-on-disk tester (CSM high temperature tribo tester). All the experiments were conducted with Al_2O_3 ball with the diameter of 6 mm in sliding contact. The tests were carried out with a load of 2 N at the linear speed of 50 mm/s and in dry sliding condition at room temperature and at the temperatures of 50 °C and 200 °C in atmospheric conditions. After the tribological tests, the images of the wear tracks were analyzed by means of SEM. Surface profiles of the wear tracks on the layers were measured by a Mitutoyo surface profilometer. The wear volume was calculated using the profiles obtained from the wear track cross-section, and thus the wear rate was attained using $K = V/(w \cdot s)$ equation, where K is the value of the wear rate, V is the worn volume, w is the normal load, and s is the distance moved.

XRD scans were performed using a Rigaku 2000 Dmax diffractometer equipment with a Cu-Kα radiation source before and after the tribological tests. The measurements were carried out between 30 and 80° scan range, and at the scan speed of 2°/min. Interpretation of the X-ray results was undertaken using JCPDS files.

3. Result and discussion

The surface morphology and thickness of MAO layers are shown in Fig. 1a and b, respectively. As shown in Fig. 1a, there were platelets indicating the formation of molten alumina that are rapidly solidified due to a quenching effect of the surrounding electrolyte on the surface [25]. Furthermore, the surface micrograph of layer clearly indicated the presence of discharge channels forming as dark circular pieces and spots dispersed all over the surface. The lamellar circular pieces were also around pores like volcano top. The cross-sectional micrography of MAO layer is shown in Fig. 1b. The micrography revealed that the MAO layer formed at unipolar mode was about 10 μm in thickness.

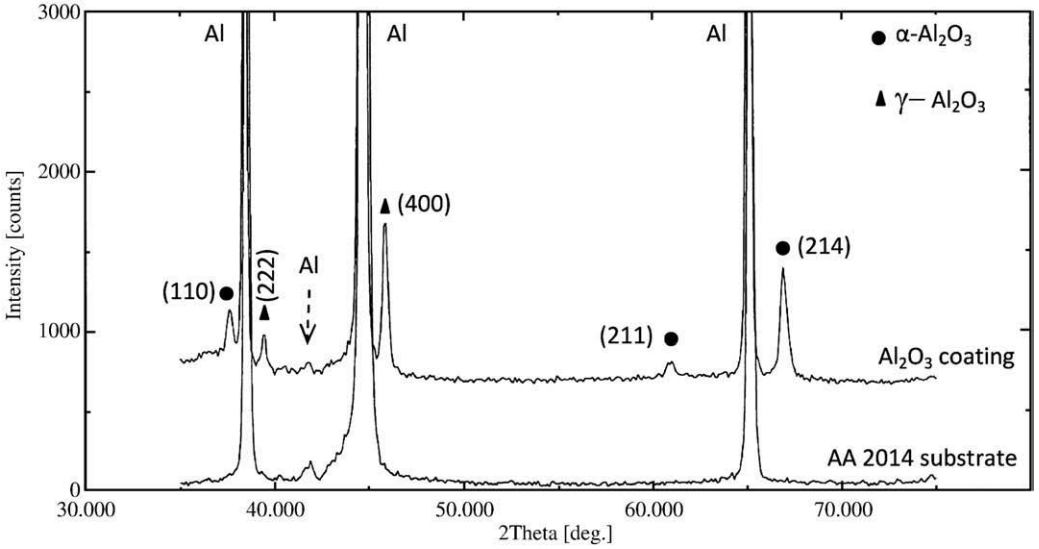

Fig. 2. XRD multiplot spectra of aluminum substrate and the MAO Al_2O_3 layers.

The layer/substrate interface was clear, and exhibited a good metallurgical adhesion between layer and substrate. It was determined that the surface roughness increased, as compare to substrate roughness. The substrate with surface roughness of Ra≈0.1 μm, increased to Ra≈0.87 μm after the MAO process. Local melting into arc channels increases and sprinkle of melted materials on surface leads to high surface roughness [26,27].

XRD analysis of MAO layers and aluminum alloy are shown in Fig. 2. The aluminum alloy substrate is composed of Al phases. The MAO layer on Al alloy is consist of α-Al_2O_3 and γ-Al_2O_3 phases (see

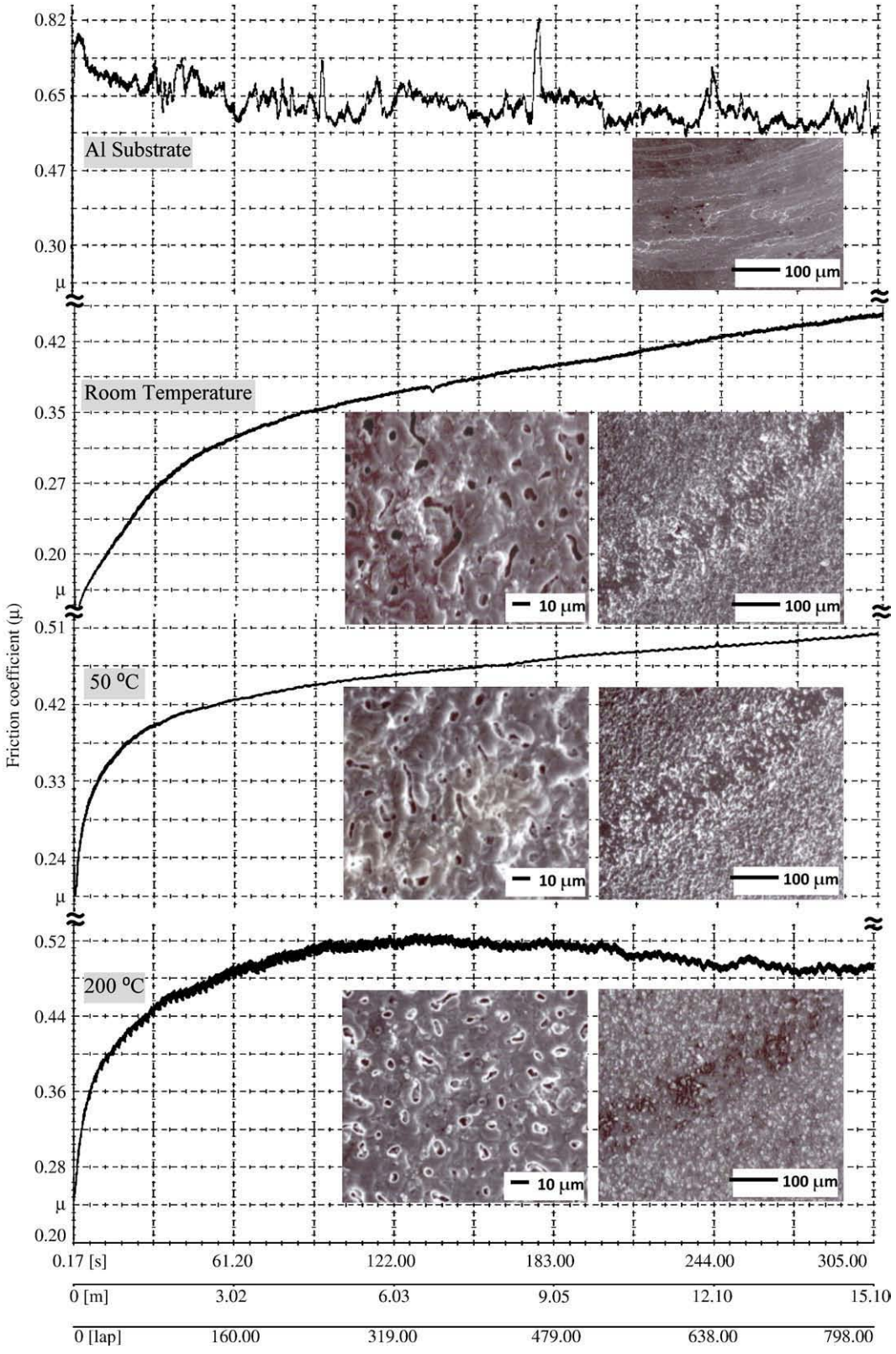

Fig. 3. The friction coefficients vs. lap, time and distance and the SEM images of the wear track and surface morphology of all the samples.

Table 2
The changes in the friction coefficients of the MAO coatings at different temperatures and aluminum substrate.

Sample	Start	Minimum	Maximum	Mean	Std.dev.
AA 2014 substrate	0.12	0,12	0.83	0.74	0.04
Wear test at room temperature	0.18	0.18	0.62	0,55	0.07
Wear test at 50 °C	0.22	0.19	0.50	0.45	0.04
Wear at 200 °C	0.25	0.24	0.52	0.39	0.03

Fig. 2). In the spectra, reflection $(214)_\alpha$ and $(400)_\gamma$ with strong diffraction intensities was identified as the diffraction peaks of α-Al_2O_3 and γ-Al_2O_3, respectively. The reflection of $(110)_\alpha$, $(211)_\alpha$ and $(222)_\gamma$ at relatively low intensity were also detected on layers. The microhardness of the layer was measured as 1200 HV. The high hardness value was related to the distribution and intensity of the hard α-Al_2O_3 phases.

The tribological tests of MAO layers were performed at room temperature and 50 °C and 200 °C. After the tribological tests, each sample was analyzed to evaluate the change on the surface morphology and phases by XRD and SEM. The wear tracks were also observed using SEM. The graphic showing the relationship between the friction coefficient and the lap, the surface morphology and the wear tracks of all MAO layers and aluminum substrate are given in Fig. 3.

Evolution of the friction coefficient with wear time, lap, and distance for the aluminum substrate and MAO layer sample under dry friction condition against Al_2O_3 ball is shown in Fig. 3. The surface morphology and wear track of layer and substrate after the tribological tests are given in same Fig. 3. Besides, Table 2 shows the minimum, maximum, mean and standard deviation of the coefficient of friction for all the samples. It was obviously seen from Fig. 3 that the friction coefficient of AA 2014 aluminum substrate was considerably unstable and approximately $\mu = 0.74$. The unstable behavior of the friction coefficient for the substrate was related to fracture of passive oxide layer under load. The graphs at room temperature and 50 °C show that the friction coefficient started low and then gradually increased during test. However, the friction force started similarly low and then remained constant with time at 200 °C. After initial stage, the increase in friction coefficient for room temperature and 50 °C resulted from abrasive effect of hard α-Al_2O_3 phases. The stable trend in friction of coefficient of sample at 200 °C can be explained with the re-modification of the surface topography, low shear force involved during sliding and the formation of a solid lubricant due to the introduction of wear debris. The change of surface topography for this temperature can be seen in Fig. 3. The pores dispersed homogeneously on the surface were obtained for 200 °C tests. On the other hand, no significant changes were seen on the surface morphologies of the specimens which were tested at room temperature and at 50 °C. Besides, it was determined that the wear test temperatures changed surface roughness of the layers. The variations on surface roughness are given in Fig. 4. There were not considerable differences at the peaks in XRD studies after the tribological tests at room temperature, 50 °C and 200 °C, as seen in Fig. 5. But the peaks

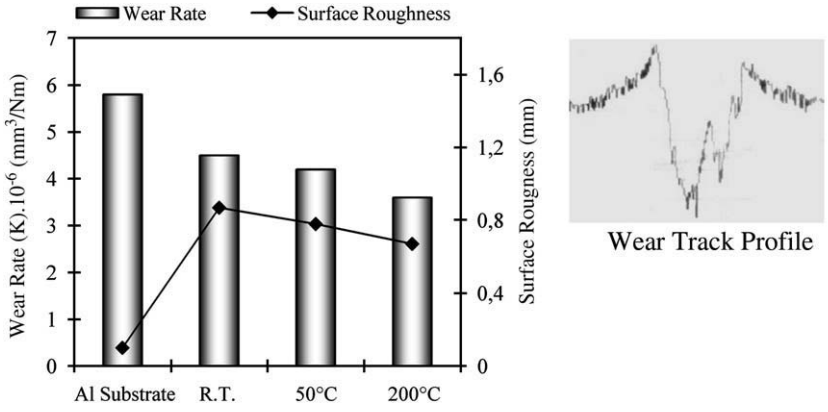

Fig. 4. The wear rates and surface roughness of all the samples and an example wear track profile.

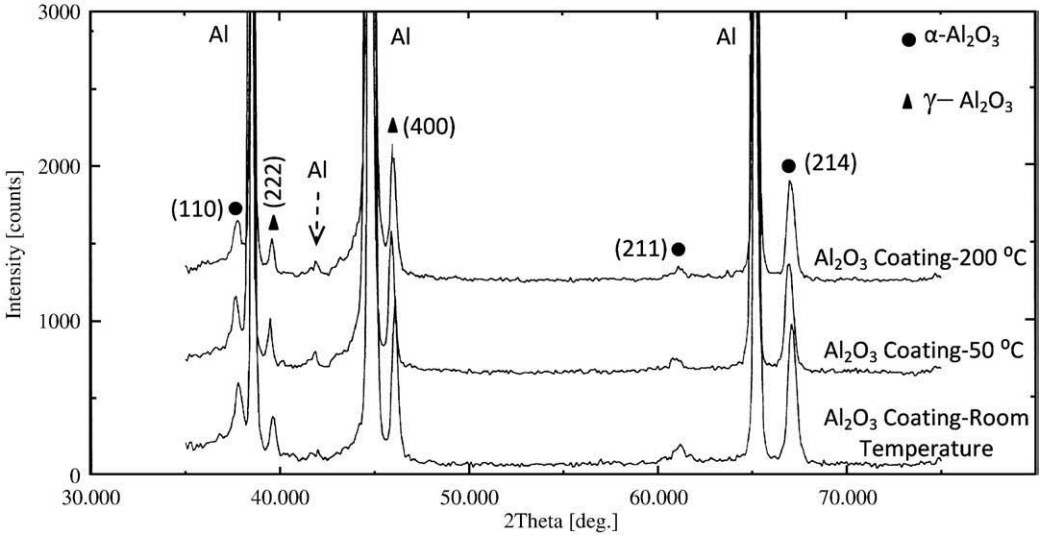

Fig. 5. XRD multiplot spectra of the layers after tribological tests.

were relatively shifted to low angles with increasing of the wear test temperature. The SEM was used to compare the wear track morphology after the tribological test at room temperature, 50 °C and 200 °C (see Fig. 3). The stable and unstable behaviour of the friction coefficients were also supported by the wear track images and wear rate. Depending on the test temperature, different values were obtained for the wear rates. The wear rates decreased with an increasing temperature. An example wear track profile and the wear rates as a graphic at different temperatures are presented in Fig. 4. The lowest wear rate was determined for the tests performed at 200 °C. The wear track images at different temperatures are given in Fig. 3. It was observed that the wear tracks at room temperature and at 50 °C were quite rough, abrasive particles and debris. On the other hand, the wear track for 200 °C was much narrower, as compared to room temperature and 50 °C. Very few fine abrasive particles were observed along the tracks for this temperature.

4. Conclusions

We conducted high temperature tribological investigation on MAO layers and studied the effects on microstructure, friction and wear of temperature. The major conclusions arising from the present study are as follows:

- The surface morphology of MAO layer is characterized by platelets indicating the formation of molten alumina, discharge channels, pores like volcano top and spots dispersed all over the surface. The surface layers of MAO layers contain of α-Al_2O_3 and γ-Al_2O_3. The high hardness values obtained for layers are correlated to α-Al_2O_3.
- It was observed that the surface morphology and roughness of the layers changed according to the wear tests carried out at different temperatures. The modifications on the surface morphology as well as the decrease in the surface roughness are achieved with increasing temperature. It was observed after the tribological tests at the temperature of 200 °C that the pores homogenously and uniformly dispersed, and volcano shaped peaks disappeared. After the tribological tests at high temperature, an apparent change was not observed for the phases that were obtained after the MAO process. While the friction coefficients exhibit a linear increase at the tribological tests carried out at room temperature and 50 °C, low friction tendency and stable friction behavior was observed at 200 °C. The wear rates decreased with increasing temperature. The lowest wear rate and narrow and smooth wear tracks are obtained at 200 °C.

Acknowledgments

The authors would like to thank the Scientific and Technological Research Council of Turkey for funding the project by grant no: MAG107M313.

References

[1] W.S. Miller, L. Zhuang, J. Bottema, A.J. Wittebrood, P. De Smet, A. Haszler, A. Vieregge, Mater. Sci. Eng. A280 (2000) 37.
[2] X. Nie, A. Leyland, H.W. Song, A.L. Yerokhin, S.J. Dowey, A. Matthews, Surf. Coat. Technol. 116–119 (1999) 1055.
[3] Fanya Jin, PaulK. Chu, Honghui Tong, Jun Zhao, App. Surf. Sci. 253 (2006) 863.
[4] A.L. Yerokhin, X. Nie, A. Leyland, A. Matthews, Surf. Coat. Technol. 122 (1999) 73.
[5] A.L. Yerokhin, X. Nie, A. Leyland, A. Matthews, Surf. Coat. Technol. 130 (2000) 195.
[6] X. Nie, A. Leyland, A. Matthews, Surf. Coat. Technol. 149 (2002) 245.
[7] Y.K. Wang, L. Sheng, R.Z. Xiong, B.S. Li, Surf. Eng. 15 (2) (1999) 109.
[8] W. Xue, Z. Deng, R. Chen, T. Zhang, Thin Solid Films 372 (2000) 114.
[9] J. Tian, Z. Luo, S. Qi, X. Sun, Surf. Coat. Technol. 154 (2002) 1.
[10] J.A. Curran, T.W. Clyne, Surf. Coat. Technol. 199 (2005) 16.
[11] A.L. Yerokhin, L.O. Snizhko, N.L. Gurevina, A. Leyland, A. Pilkington, A. Matthews, Surf. Coat.Technol. 177–178 (2004) 779.
[12] R.C. Barik, J.A. Wharton, R.J.K. Wood, K.R. Stokes, R.L. Jones, Surf. Coat. Technol. 199 (2005) 158.
[13] J.A. Curran, H. Kalkancı, Yu. Magurova, T.W. Clyne, Surf. Coat. Technol. 201 (21) (2007) 8683.
[14] T. Wei, F. Yan, J. Tian, J. Alloys Compd. 389 (2005) 169.
[15] P.I. Butyagin, Ye.V. Khokhryakov, A.I. Mamaev, Mater. Lett. 57 (2003) 1748.
[16] Y. Wang, T. Lei, B. Jiang, L. Guo, Appl. Surf. Sci. 233 (2004) 258.
[17] A.L. Yerokhin, V.V. Lyubimov, R.V. Ashitkov, Ceram. Int. 24 (1998) 1.
[18] G. Yang, X. Lü, Y. Bai, H. Cui, Z. Jin, J. Alloys Compd. 345 (2002) 196.
[19] X. Wenbin, W. Chao, L. Yongliang, D. Zhiwei, C. Ruyi, Z. Tonghe, Mater. Lett. 56 (2002) 737.
[20] X. Sun, Z. Jiang, S. Xin, Z. Yao, Thin Solid Films 471 (2005) 194.
[21] A.L. Yerokhin, A. Leyland, A. Matthews, Appl. Surf. Sci. 200 (2002) 172.
[22] W. Xue, C. Wang, R. Chen, Z. Deng, Mater. Lett. 52 (6) (2002) 435.
[23] W. Xue, Z. Deng, R. Chen, T. Zhang, Thin Solid Films 372 (2000) 114.
[24] M.H. Zhu, Z.B. Cai, X.Z. Lin, P.D. Ren, J. Tan, Z.R. Zhou, Wear 263 (2007) 472.
[25] W. Xue, Z. Deng, R. Chen, T. Zhang, H. Ma, J. Mater. Sci. 36 (2001) 2615.
[26] A.L. Yerokhin, L.O Snizhko, N.L Gurevina, A. Leyland, A. Pilkington, A. Matthews, J. Phys. D 36 (2003) 2110.
[27] N. Parvini Ahmadi, R.A. Khosroshahi, B. Baghal, Asian J. Appl. Sci. (2008) 1.